Earth and Planetary Science Letters 290 (2010) 427–437

Contents lists available at ScienceDirect

Earth and Planetary Science Letters

journal homepage: www.elsevier.com/locate/epsl

Glacial effects on weathering processes: New insights from the elemental and lithium isotopic composition of West Greenland rivers

Josh Wimpenny [a,*], Rachael H. James [a,1], Kevin W. Burton [a,2], Abdelmouhcine Gannoun [a,3], Fatima Mokadem [a,2], Sigurður R. Gíslason [b]

[a] Dept. of Earth and Environmental Science, The Open University, Milton Keynes MK7 6AA, UK
[b] Institute of Earth Sciences, University of Iceland, Sturlugata 7, 101 Reykjavik, Iceland

ARTICLE INFO

Article history:
Received 8 June 2009
Received in revised form 14 December 2009
Accepted 30 December 2009
Available online 20 January 2010

Editor: M.L. Delaney

Keywords:
lithium isotopes
glacial weathering
Greenland
weathering fluxes

ABSTRACT

Greenland is by far the dominant source of glacial runoff to the oceans but the controls on the chemical and isotopic composition of this runoff are poorly known. To better constrain glacial effects on weathering processes, we have conducted elemental and lithium isotope analyses of glacial and non-glacial rivers in gneiss catchments in West Greenland. The glacial rivers have high total suspended solids (0.5 g l^{-1}) and low total dissolved solids (12 μScm^{-1}) relative to the non-glacial rivers, and they contain a higher proportion of dissolved Ca^{2+} and K^{+} because of subglacial, preferential, weathering of trace carbonates and biotite. The glacial rivers also have high SO_4^{2-} because of the oxidation of trace sulphides under the ice. Both glacial and non-glacial rivers have high δ^7Li (respectively, ~26‰ and ~30‰) relative to the rocks from which the Li is derived (~8‰). Saturation state modelling suggests that this is due to the formation of Fe-oxyhydroxides in the non-glacial rivers, with preferential uptake of ^{6}Li during inner sphere sorption of Li^{+} on the Fe-oxyhydroxide surface. Glacial rivers, however, are undersaturated with respect to clay minerals and Fe-oxyhydroxides. Nevertheless, leaching of suspended sediments indicates that ~65% of the Li in these sediments is associated with Fe-oxyhydroxide phases, and the δ^7Li value of this Li is low, ~5‰. These results suggest that these Fe-oxyhydroxides formed under the ice, as a product of sulphide oxidation, with preferential uptake of ^{6}Li onto the mineral surface. Solubilisation of Li from these Fe-oxyhydroxide phases is unlikely to represent a significant flux of Li to the oceans. Moreover, because the difference between the δ^7Li values of glacial vs non-glacial rivers is small, glaciation has not had a significant impact on the Li isotopic composition of the riverine flux delivered to the oceans in the past, even at the height of the last deglaciation.

1. Introduction

The chemical weathering of continental silicate rocks results in drawdown of carbon dioxide from the Earth's atmosphere which, in turn, regulates Earth's climate (Walker et al., 1981; Berner et al., 1983). In general the rates of chemical weathering increase with temperature [e.g. (White and Blum, 1995)], providing a crucial feedback mechanism between weathering and climate. However, studies of glacier-covered alpine catchments have yielded chemical weathering rates far greater than the global average (Sharp et al., 1995; Jacobson and Blum, 2003), which has led to speculation that glacial weathering can cause significant atmospheric CO_2 drawdown (Sharp et al., 1995). On the other hand, other studies suggest that glacial solute fluxes are largely derived from non-silicate sources (Anderson et al., 1997) which have little effect on the long-term carbon cycle.

Nevertheless, what is clear is that glacial sediments are particularly susceptible to chemical weathering because of their high surface area per unit mass and the strained minerals produced by abrasion (Petrovich, 1981), and that glacial weathering processes impart a compositionally distinct chemical signal to the oceans. Glacial runoff is generally more dilute than the global mean river water, and usually contains proportionally more K^{+} because of preferential weathering of biotite, and less Si because silicate weathering rates are depressed (Anderson et al., 2000). Moreover, the proportion of Ca^{2+} is high, even for Si-rich igneous and metamorphic bedrocks (Raiswell and Thomas, 1984), because of preferential weathering of trace carbonates, and the proportion of SO_4^{2-} is high because of oxidation of trace sulphides under the ice [e.g.(Tranter, 2003)].

Lithium (Li) and lithium isotopes have the potential to provide important new information on the mineral reactions that occur during chemical weathering and thus control river chemistry in both glacial

* Corresponding author. Geology Department, University of California, One Shields Avenue, Davis, CA, 95616, United States.
E-mail address: jbwimpenny@ucdavis.edu (J. Wimpenny).
[1] Now at: National Oceanography Centre Southampton, Southampton SO14 3ZH, UK.
[2] Now at: Dept. of Earth Sciences, Oxford University, Oxford OX1 3PR, UK.
[3] Now at: Laboratoire Magmas et Volcans, OPGC, UBP, UMR6524, 5 Rue Kessler 63038 Clermont Ferrand Cedex, France.

0012-821X/$ – see front matter © 2010 Elsevier B.V. All rights reserved.
doi:10.1016/j.epsl.2009.12.042

and non-glacial environments. This is because while Li isotopes are unaffected during the dissolution of primary minerals [e.g. (Pistiner and Henderson, 2003)], or by biomass uptake, they are strongly fractionated by the formation of secondary minerals (Huh et al., 1998; Pistiner and Henderson, 2003; Kisakurek et al., 2004; Chan and Hein, 2007). Lithium is retained in clays including smectite (Vigier et al., 2008) and illite (Williams and Hervig, 2005), as well as in oxide minerals such as gibbsite (Pistiner and Henderson, 2003) and goethite (Chan and Hein, 2007). The lighter Li isotope, ^{6}Li, is incorporated in preference to ^{7}Li, leaving the fluid phase enriched in ^{7}Li. As a result, the Li isotope composition of river water [δ^{7}Li ~23‰, (Huh et al., 1998)] is heavier isotope composition than that of the rock from which the Li is derived (Huh et al., 2001; Kisakurek et al., 2005). For this reason, the principal control on the Li isotopic composition of riverwater is not catchment lithology; rather, it is largely regulated by the extent of secondary mineral formation and thus weathering intensity (Kisakurek et al., 2005).

The aim of this study is to characterise the chemical and Li isotope composition of both glacially sourced and non-glacial rivers in West Greenland. Crucially, studies of the chemical composition of streams emanating from the Greenland ice sheet are scarce (Yde et al., 2005) yet glacial runoff provides 0.6–1% of the global average runoff and Greenland is by far the dominant source (Tranter, 2003). Moreover, because of global warming, glacial fluxes are set to increase, which may have major implications not only for the geochemical cycles of some elements (van de Flierdt et al., 2002), but also for thermohaline circulation which is driven by freshwater inputs to the North Atlantic Ocean [e.g. (Bryden et al., 2005)].

To this end, we present comprehensive elemental concentration and Li isotope data for both glaciated and non-glaciated river systems in West Greenland. The river catchments are essentially monolithological, so the data can be used to: (1) identify the mechanisms that regulate chemical weathering in glacial versus non-glacial regimes; (2) explore the behaviour of Li and Li isotopes during glacial weathering; and (3) evaluate the significance of the glacially-influenced riverine flux of trace elements and Li isotopes to the oceans and the Li oceanic geochemical cycle.

2. Geology, climate and river settings

Greenland has a surface area of 2 166 086 km^2, of which the Greenland ice sheet covers 1 730 000 km^2 or 81% (Tranter, 2003). The geology of Greenland is dominated by crystalline rocks that formed during successive orogenic events in the Archean and early Proterozoic and stabilised as Precambrian shield around 1600 Ma (Escher and Pulvertaft, 1995). The rivers sampled in this study are located in the vicinity of the town of Kangerlussuaq in the southwest of Greenland (Fig. 1); this area is formed of essentially monolithological Archean gneiss that has been metamorphosed to amphibolite facies. The climate in the region is Arctic; the mean annual temperature is −5 °C and the area is underlain by continuous permafrost (Jorgensen and Andreasen, 2007). However, due to its continental location, temperature varies widely over the course of the year; in winter, temperatures can be as low as −50 °C while summers can be relatively mild with temperatures exceeding 20 °C (Russell, 2007). Kangerlussuaq sits in a region of negative precipitation, where evaporation exceeds precipitation by ~150 mm each year. The high level of evaporation means that numerous saline lakes have developed at the head of the Kangerlussuaq fjord (Anderson et al., 1999).

River samples were taken in July 2006 from both 'glacial' and 'non-glacial' rivers. For the purposes of this study, glacial rivers refer to those that are directly fed by ice sheet melting, while non-glacial rivers refer to rivers that are not directly linked to the ice sheet. Glacial river water was sampled from both of the major rivers in the region, Akuliarusiarsuup Kuua and Quinnguata Kuusua, which merge at Kangerlussuaq to form the Watson River. It is important to note that 'glacial' samples include not only those collected adjacent to the ice sheet (GR1 and GR9), but also samples collected downstream of the ice sheet (e.g. GR5). These samples will have mixed to some extent with non-glacially sourced water. Nevertheless, the flux of water delivered by non-glacial tributaries is low relative to that sourced directly from the ice sheet. Non-glacial river waters were taken from a variety of streams and small rivers, some of which were coloured (GR11 and GR12), possibly reflecting a high organic content. Non-glacial river discharge is derived from direct precipitation as well as from shallow lakes, which make up 5–10% of the surface area around Kangerlussuaq (Willemse, 2002). The water balance in these lakes is controlled by direct precipitation, spring melting of the snowpack and evaporative loss (Willemse, 2002). Overland flow from the ice sheet to the lakes is limited and, although subsurface mixing between glacial and non-glacial waters is possible, this should be kept to a minimum by a continuous layer of permafrost in the Kangerlussuaq region (Jorgensen and Andreasen, 2007). One sample (GR3) was taken from up on the ice sheet itself; because this stream originates from superficial melting of the ice sheet it is described as being supraglacial. Sample GR10 was taken from close to the harbour and contains a significant seawater component; for this reason it is not referred to in the discussion of non-glacial samples. Sample GR14 (not shown on Fig. 1) was taken from close to the town of Sisimiut, to the north of the main study region.

3. Field and analytical techniques

3.1. Sample collection and preparation

Samples of river water, suspended sediment and bedload were collected at each sample site. In situ measurements of pH and temperature were performed using a Hanna Instruments pH meter with a precision of 0.1 pH units and 0.1 °C and accuracy (at 20 °C) of ±0.01 pH units, and ±0.5 °C. Measurements of total dissolved solids (TDS) were performed using a handheld Hanna Instruments TDS meter with a precision and accuracy of 0.1 μScm^{-1} and ±1%, respectively. Both instruments were calibrated prior to sample collection using standard pH and conductivity solutions. Around 100 ml of river water was hand-pumped through a preweighed filter (0.2 μm), which was carefully stored for later weighing. A further ~10 l of water was collected and filtered (0.2 μm) using a pressurised PTFE unit within 12 h of sampling; the suspended sediment on the filters was stored while filtered water was retained either for later analysis or further filtration. The alkalinity of each water sample was determined soon after filtration by titrating against 0.01 M HCl. Alkalinity was calculated from the Gran function, on the basis that the concentration of H^+ increases linearly as a function of the volume of acid added as soon as all HCO_3^- has been converted to H_2CO_3 (Appelo and Postma, 2005). The alkalinity of the sample is given by the equivalence point which is reverse extrapolated from the linear part of the Gran plot. Between 5 and 10 l of the 0.2 μm filtered water was then filtered at 10 kD through a tangential ultrafiltration system. Ultrafiltration prevents particles larger than 10 kD from passing through the filter membrane so the residual solution comprises a mixture of the initial 0.2 μm filtrate and colloids (<0.2 μm, >10 kD). Meanwhile the filtrate contains only truly dissolved material (<10 kD). The ultrafiltration process was continued until ~250 ml of residual solution remained.

On return from the field the hand pump filters were dried at 40 °C overnight and reweighed to ascertain the concentration of total suspended sediment (TSS) in the river water. Bedload sediments were dried and crushed to a fine powder using an agate mill. Sub-samples (~0.1 g) of the powdered bedload and suspended sediment were dissolved in a mixture of thermally-distilled (TD) HNO_3 and HF and, after drying, the final sample was redissolved in 2% TD HNO_3 for

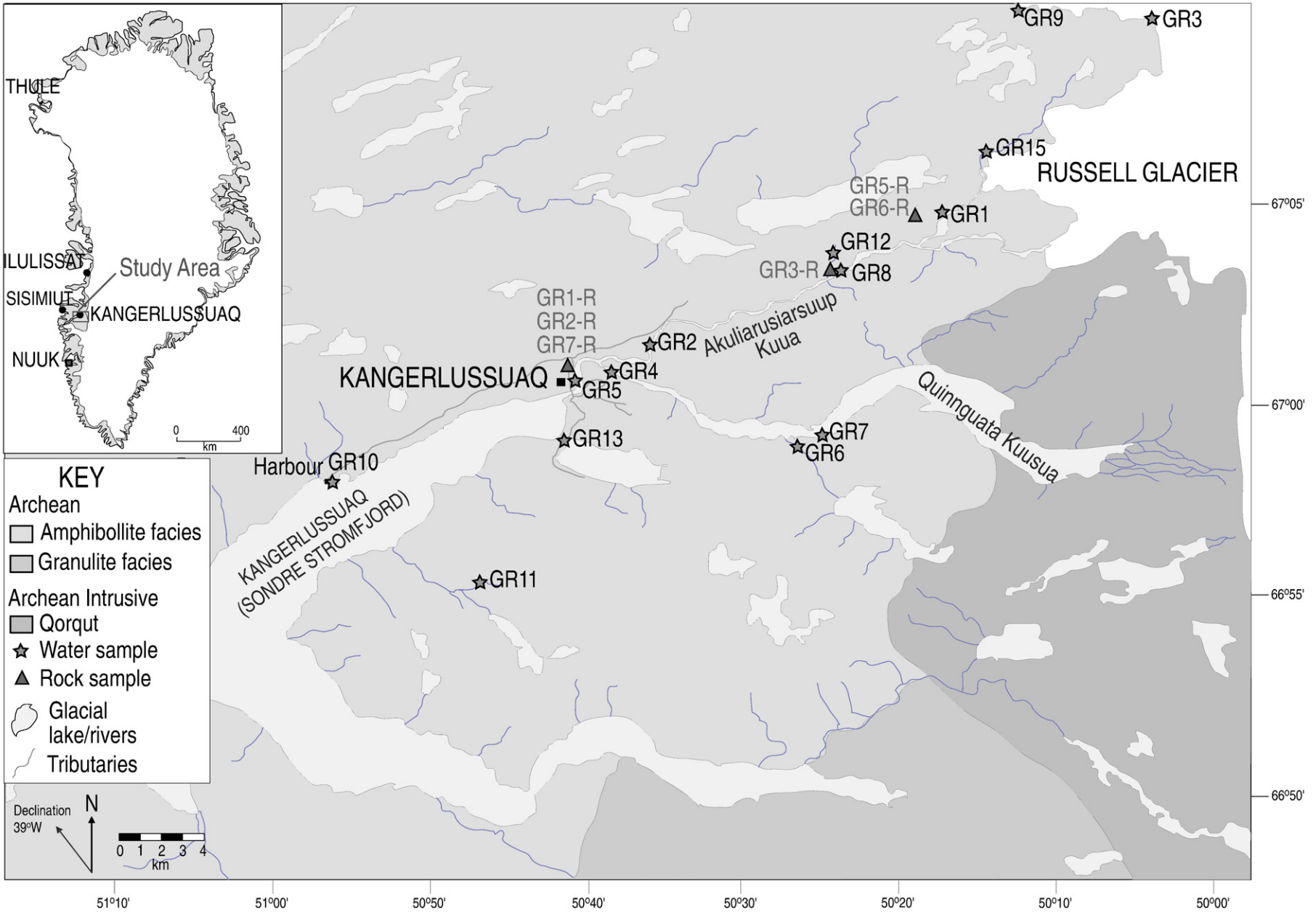

Fig. 1. Location map showing the water and rock sampling sites and geology underlying the Kangerlussuaq region of SW Greenland.

analysis by an inductively coupled plasma mass spectrometer (ICP-MS). A number of rock standards were also prepared using this technique for use as calibration standards for ICP-MS analyses.

3.2. Cation and anion analyses

Concentrations of major elements in the bedload and rock samples were determined by X-ray fluorescence (XRF) with reference standards reproducing to within 1% of certified values. Cation concentrations in the suspended sediment, dissolved load and colloids were determined by ICP-MS. River waters and colloids were calibrated against multi element standards of known concentration and corrected for machine drift by repeat measurements of the in-house riverwater standard Sco2/15. The external reproducibility of these analyses was calculated from repeat measurements of the river water standard SLRS-4 and is better than $\pm 8\%$ (2σ; $n=15$) for all elements.

Rock and sediment samples were calibrated against the certified reference materials JB-2, BIR-1, BCR-2, JG-2, SDC-1 and AGV-1. One of these standards was also measured repeatedly during each sample run to correct for machine drift. Two standards (BIR-1 and JB-2) were routinely measured to calculate the external reproducibility of this technique; this is better than $\pm 6\%$ (2σ; $n=14$) for all major and minor elements.

The concentration of dissolved anions was determined by ion chromatography, with an uncertainty of better than $\pm 10\%$ (2σ).

3.3. Leaching experiment

Sub-samples (~0.2 g) of three of the suspended sediment samples from glacial rivers were subjected to a two stage acid leaching process similar to that described by Chan and Hein (2007). First, the samples were leached in buffered acetic acid (pH = 4.6) to remove exchangeable cations, and they were then leached in 2 N TD HCl to remove cations bound to iron and manganese oxyhydroxides. The chemical composition of the leachates was determined by ICP-MS; lithium isotope ratios were determined by multi-collector (MC) ICP-MS (Section 3.4).

3.4. Li isotope analyses

Samples containing at least 10 ng of Li were passed through a cation exchange column in order to separate the Li from the sample matrix (James and Palmer, 2000). Isotope measurements were performed by MC-ICP-MS, using a sample-standard bracketing technique, relative to the L-SVEC standard (Flesch et al., 1973). Isotope ratios are presented as δ^7Li, in per mil variations from L-SVEC:

$$\delta^7\mathrm{Li} = \left\{ \frac{\left(\frac{^7\mathrm{Li}}{^6\mathrm{Li}}\right)_{\mathrm{Sample}}}{\left(\frac{^7\mathrm{Li}}{^6\mathrm{Li}}\right)_{\mathrm{LSVEC}}} - 1 \right\} \times 1000$$

The internal precision of the analyses was typically better than 0.1‰ (2σ). The external reproducibility was determined by repeat measurements of IAPSO seawater. The average of 40 analyses gave a δ^7Li value of 31.08 ± 0.82‰ (2σ).

4. Results

Data for pH, temperature, alkalinity, TDS and total suspended solids (TSS) are given in Table 1. Concentrations of major and minor cations, anions, and Li isotope data for the dissolved, ultrafiltered and colloidal phases are given in Table 2. Cation concentration and Li isotope data for the solid phases are given in Table 3.

4.1. In situ measurements

Concentrations of TDS and TSS are distinctly different in the glacially and non-glacially sourced rivers. Glacial rivers have low TDS (2.6–18 μScm^{-1}) and high TSS (0.23–0.85 g/l) while non-glacial rivers have high TDS (25–198 μScm^{-1}) and low TSS (0.002–0.014 g/l). In the glacial rivers TDS, TSS and alkalinity all increase with distance from the ice sheet. The pH of most of the rivers lies between 7 and 8 but sample GR3, which is a supraglacial river, has a relatively low pH (6.3).

4.2. Major and trace elements

4.2.1. Dissolved load

As a percentage of the sum of the major cations ($Na^+ + Mg^{2+} + Ca^{2+} + K^+$), Ca^{2+} dominates the dissolved load of both glacial and non-glacial rivers (57 and 44% respectively, Fig. 2). Glacial rivers have relatively more K^+ (~12%) and less Mg^{2+} (~16%) than non-glacial rivers (which have ~5% K^+ and ~36% Mg^{2+}), but the proportion of Na^+ is similar (~16%). Concentrations of dissolved Si are variable, ranging from 6.1 to 42 μmol/l in glacial rivers and up to 323 μmol/l in non-glacial rivers. Iron concentrations in the dissolved load are between 87 and 690 nmol/l in glacial rivers, compared to between 170 and 12,700 nmol/l in non-glacial rivers. All but two rivers (GR11 and GR12) have iron concentrations lower than the global average (1180 nmol/l; (Gaillardet et al., 2003). Anions consist almost entirely

Table 1
Field measurements for Greenland river samples. n.d. = not determined.

Sample	Latitude	Longitude	Origin	pH	T (°C)	TDS (μScm^{-1})	TSS (g/l)	Alkalinity (meq/l)
GR1	N 67°04.666′	W 50°16.935′	Glacial	8.48	4.2	9.21	0.435	0.073
GR2	N 67°01.745′	W 50°35.683′	Glacial	7.91	4.2	14.4	0.598	0.098
GR3	N 67°09.129′	W 50°02.790′	Supraglacial	6.32	0.6	2.6	0.229	0.023
GR4	N 67°01.057′	W 50°39.869′	Glacial	7.11	6	17.8	0.846	0.119
GR5	N 67°01.172′	W 50°40.747′	Glacial	7.18	3	9.77	0.399	0.145
GR6	N 66°59.057′	W 50°27.051′	Non-glacial	7.61	12.62	61.6	n.d.	0.133
GR7	N 66°59.243′	W 50°26.962′	Glacial	7.3	8.6	12.7	0.545	0.151
GR8	N 67°03.269′	W 50°24.644′	Glacial	7.2	5.5	10.7	0.444	0.099
GR9	N 67°09.060′	W 50°13.101′	Glacial	7.18	5.3	6.77	n.d.	0.266
GR10	N 66°58.09′	W 50°57.101′	Fjord	6.96	10.5	2650	0.162	0.358
GR11	N 66°55.915′	W 50°46.448′	Non-glacial	6.81	10	25.1	0.004	1.74
GR12	N 67°03.606′	W 50°25.983′	Non-glacial	8.3	19.3	198	0.014	0.532
GR13	N 66°59.089′	W 50°41.864′	Non-glacial	7.65	14.2	55.3	n.d.	0.556
GR14	N 66°57.096′	W 53°39.940′	Non-glacial	8.1	7.5	120	0.002	0.784
GR15	N 67°05.945′	W 50°15.950′	Non-glacial	8.25	12.3	106	n.d.	0.073

Table 2
Anion, cation and Li isotope data for the dissolved, ultrafiltered and colloidal phases from the Greenland Rivers. n.d. = not determined.

	Anions (μmol/l)			Major cations (μmol/l)						Minor cations (nmol/l)			δ^7Li (‰)
	HCO_3^-	Cl^-	SO_4^{2-}	Si	Al	Na	Ca	Mg	K	Fe	Sr	Li	
Dissolved (<0.2 μm)													
GR1	72.8	1.95	8.29	19.6	1.64	11.6	24.8	8.28	12.2	229	59.6	49.1	25.4
GR2	98.5	5.97	13.4	21.6	0.73	29.9	32.9	11.0	18.2	117	58.6	68.7	26.6
GR3	23.3	1.75	7.06	6.14	0.10	2.99	11.1	3.3	4.54	55.6	15.7	14.3	13.5
GR4	119	4.31	19.5	25.7	0.57	32.2	40.8	11.6	20.2	87.0	66.9	75.3	25.3
GR5	145	5.15	16.8	24.8	0.72	30.2	39.2	11.4	18.6	99.0	64.4	67.5	26.7
GR7	133	4.13	19.3	28.7	1.08	35.4	42.4	13.7	21.6	132	73.0	91.2	25.6
GR8	151	3.18	17.9	42.1	5.34	37.7	40.6	14.4	22.9	693	77.8	91.6	25.4
GR9	99.3	n.d.	10.7	21.7	1.18	8.01	31.1	9.71	9.75	177	53.8	31.4	25.9
GR10	266	42,300	1890	26.6	0.71	>2000	615	2940	586	428	5050	1810	30.4
GR11	358	94	17.2	76.1	3.40	99.1	105	86.3	15.6	1440	307	50.6	27.1
GR12	1740	596	263	323	8.62	539	665	775	142	12,700	1070	569	36.5
GR13	532	105	22	6.88	0.77	136	148	116	40.5	179	441	82.8	30.8
GR14	556	324	72	59.5	0.53	362	229	91.1	11.2	250	1150	14.3	24.5
GR15	784	119	28.4	4.17	0.08	171	181	202	82.7	174	285	195	29.3
Ultrafiltered (<10 kD)													
GR1	n.d.	n.d.	n.d.	n.d.	0.04	30.9	16.8	8.90	9.90	<2	39.0	44.3	n.d.
GR2	n.d.	n.d.	n.d.	n.d.	0.10	28.8	24.8	9.50	16.4	<2	55.9	72.9	n.d.
GR4	n.d.	n.d.	n.d.	n.d.	0.09	30.7	32.8	10.8	17.0	<2	61.0	61.4	n.d.
GR5	n.d.	n.d.	n.d.	n.d.	0.09	29.2	29.7	10.2	16.0	<2	56.3	64.3	n.d.
GR7	n.d.	n.d.	n.d.	n.d.	n.d.	32.5	32.7	10.8	19.2	<2	65.3	81.4	22.9
GR8	n.d.	n.d.	n.d.	n.d.	n.d.	n.d.	n.d.	n.d.	n.d.	n.d.	n.d.	n.d.	24.0
GR10	n.d.	n.d.	n.d.	n.d.	0.73	>2000	621	2790	605	754	4790	1620	n.d.
GR11	n.d.	n.d.	n.d.	n.d.	0.65	73.7	75.3	69.3	13.5	218	242	44.3	n.d.
GR12	n.d.	n.d.	n.d.	n.d.	2.96	543	465	646	139	950	860	511	35.4
GR13	n.d.	n.d.	n.d.	n.d.	0.60	133	123	110	40.4	84.3	417	78.6	31.4
GR14	n.d.	n.d.	n.d.	n.d.	0.35	355	193	86.2	11.1	133	1067	15.7	n.d.
GR15	n.d.	n.d.	n.d.	n.d.	0.07	175	156	198	82.6	164	289	184	27.2
Colloids (<0.2 um, >10 kD)													
GR1	n.d.	n.d.	n.d.	n.d.	12.0	55.1	56.2	25.1	24.3	2500	217	69.5	16.6
GR2	n.d.	n.d.	n.d.	n.d.	7.20	43.3	58.2	20.4	28.2	2350	182	116	16.4
GR4	n.d.	n.d.	n.d.	n.d.	14.8	45.2	63.2	22.7	27.5	4240	195	99.4	21.7
GR5	n.d.	n.d.	n.d.	n.d.	16.1	47.0	69.6	24.4	29.6	4430	217	101	20.9
GR7	n.d.	n.d.	n.d.	n.d.	47.4	66.8	97.7	39.5	45.1	13,900	353	157	13.2
GR8	n.d.	n.d.	n.d.	n.d.	n.d.	n.d.	n.d.	n.d.	n.d.	n.d.	n.d.	n.d.	17.9
GR10	n.d.	n.d.	n.d.	n.d.	0.30	>2000	607	2710	564	416	6350	1920	n.d.
GR11	n.d.	n.d.	n.d.	n.d.	42.1	69.2	266	158	15.5	37,000	1160	64.3	n.d.
GR12	n.d.	n.d.	n.d.	n.d.	68.1	668	1820	1630	189	352,000	4390	734	35.2
GR13	n.d.	n.d.	n.d.	n.d.	1.70	150	221	149	47.4	2430	977	95.9	30.3
GR14	n.d.	n.d.	n.d.	n.d.	2.10	407	332	120	13.0	3370	2460	16.6	n.d.
GR15	n.d.	n.d.	n.d.	n.d.	0.30	197	272	258	102	953	671	226	29.1

of bicarbonate, sulphate and chloride. The dominant anion is always HCO_3^- (~72%) while the importance of Cl^- and SO_4^{2-} varies between the glacial and non-glacial rivers. Glacial rivers have low Cl^- and high SO_4^{2-} (~3 and ~22% respectively) while non-glacial rivers have high Cl^- and low SO_4^{2-} (~20 and ~10% respectively). Nitrate is present in samples GR11 and GR12 but it is below the detection limit (0.1 ppm) in all other samples.

4.2.2. Colloidal and ultrafiltered fractions

Comparison of concentrations in the dissolved (<0.2 μm) and ultrafiltrated (<10 kD) fractions (Table 2) shows that the removal of colloids (<0.2 μm, >10 kD) from the dissolved phase greatly reduces levels of Fe and Al while the concentrations of other elements is relatively unaffected (e.g. Li, Na, and Mg). Mass balance calculations indicate that some loss of Fe (~20%) and Al (~30%) occurred during the ultrafiltration process, consistent with the fixation of Fe and Al-oxyhydroxides to the filtration cassette (Dupre et al., 1999; Riotte et al., 2003). Consequently, the colloidal fraction (<0.2 μm, >10 kD) is depleted in Fe and Al, but the concentrations in the ultrafiltrated fraction (<10 kD) are unaffected. The ultrafiltrated concentrations indicate that almost all of the Fe in the <0.2 μm fraction from glacial rivers is colloidal, as is ~90% of Al. The importance of colloids is more variable in non-glacial rivers; colloids contain 5–47% of the iron and 12–81% of the aluminium in the <0.2 μm fraction. There appears to be little colloidal K in non-glacial rivers although ~14% of the K in glacial rivers is in colloidal form, whereas some (~25%) of the Ca in the <0.2 μm fraction in both types of river is colloidal.

4.2.3. Solid phases

A wide selection of rock types were sampled and analysed during this study but not all are representative of the dominant lithologies in the Kangerlussuaq region. Samples GR2R and GR6R appear to be closest in composition to average Greenland amphibolite, according to data compiled by Wells (1979). The chemical composition of the bedload is similar in glacial and non-glacial rivers and close to the average chemical composition of the bedrock. The average Si concentration of both the bedrock and bedload is ~31 wt.%. However, the chemical composition of the suspended sediment (available only for the glacial rivers) is distinctly different from the bedload and bedrock; the suspended sediments are enriched in Ca, Mg, K, and Fe but generally have lower Al.

4.3. Leaching experiments

The acetic acid leach of the suspended particles removed <5% of the total available Li, Na, Mg, K, Ca, Fe and Sr. By contrast, almost all of

Table 3
Cation concentrations for the solid phases from Greenland rivers (SP = suspended sediment, S = bedload and R = bedrock). *Amphibolite data is from Wells (1979) n.d. = not determined.

Samples	Major cations (wt.%)							Minor cations (ppm)		δ^7Li (‰)
	Si	Al	Na	Ca	Mg	K	Fe	Sr	Li	
GR1-SP	n.d.	6.95	2.47	3.12	2.07	2.15	5.07	374	35.2	2.95
GR2-SP	n.d.	6.86	2.59	3.13	1.69	2.17	4.30	407	29.2	3.58
GR3-SP	n.d.	6.53	2.54	3.09	1.79	1.76	4.46	378	25.2	3.89
GR4-SP	n.d.	6.86	2.66	3.17	1.85	2.05	3.90	393	24.9	3.12
GR5-SP	n.d.	6.94	2.83	3.24	1.74	1.95	3.68	396	21.5	3.62
GR7-SP	n.d.	6.77	2.59	3.15	1.92	2.08	4.01	387	26.8	3.63
GR8-SP	n.d.	6.90	2.56	3.12	2.12	2.17	4.09	376	29.1	3.11
GR9-SP	n.d.	7.21	2.66	3.12	1.97	2.34	4.57	392	35.4	2.73
GR10-SP	n.d.	6.70	2.53	3.28	2.07	1.65	4.79	389	30.3	4.00
GR1-S	32.3	7.36	2.82	2.49	0.99	1.42	3.20	388	8.72	5.58
GR2-S	33.2	7.32	2.87	2.26	0.80	1.38	2.67	396	9.27	4.80
GR3-S	32.0	7.27	2.70	2.45	1.17	1.11	4.07	375	10.3	3.95
GR4-S	29.9	6.77	2.33	2.53	1.44	1.15	7.09	325	10.8	5.02
GR5-S	32.0	7.22	2.74	2.48	1.20	1.33	3.87	375	10.3	4.96
GR7-S	32.0	7.72	2.96	2.54	1.14	1.52	3.11	414	10.2	5.17
GR8-S	33.7	6.91	2.76	1.86	0.65	1.62	2.25	358	9.82	5.60
GR9-S	30.4	7.12	2.73	2.40	1.18	1.06	4.93	412	11.1	6.91
GR10-S	31.4	7.27	2.77	2.37	1.22	1.59	3.78	361	13.5	5.43
GR11-S	32.4	7.22	2.84	2.21	1.06	1.44	2.73	335	13.2	3.94
GR12-S	30.7	6.41	2.35	2.17	0.94	1.24	5.44	310	9.64	5.64
GR13-S	33.5	7.07	2.78	2.02	0.83	1.51	2.50	362	9.62	4.95
GR14-S	32.4	6.73	2.50	2.57	1.36	0.74	3.35	486	11.1	3.77
GR15-S	31.0	7.20	2.73	2.57	1.24	1.36	3.29	344	11.1	3.64
GR1-R	26.1	7.62	1.14	5.66	4.35	0.74	6.64	155	11.4	9.46
GR2-R	31.1	7.27	2.60	2.41	1.93	2.13	3.22	434	24.9	5.77
GR3-R	24.7	6.75	1.77	4.64	3.11	1.28	9.91	186	15.2	9.59
GR5-R	23.8	5.05	0.79	4.70	9.16	0.64	8.23	88.0	26.2	10.4
GR6-R	33.0	7.83	3.35	1.15	0.71	2.25	1.71	413	11.3	7.34
GR-KISS	23.5	6.75	1.75	5.03	2.90	0.56	12.2	146	17.7	10.4
Mean amphibolite*	31.3	8.34	3.53	2.18	0.88	1.79	2.14			

the iron in the suspended sediments was removed by leaching in 2 M HCl, along with ~65% of the Li, ~19% of the Na, ~3% of the K, ~45% of the Ca and ~15% of the Sr.

4.4. Lithium and lithium isotopes

The Li concentration in the bedrock ranges from 11 to 26 ppm, and δ^7Li values range from 5.8 to 10.4‰. In comparison the bedload has

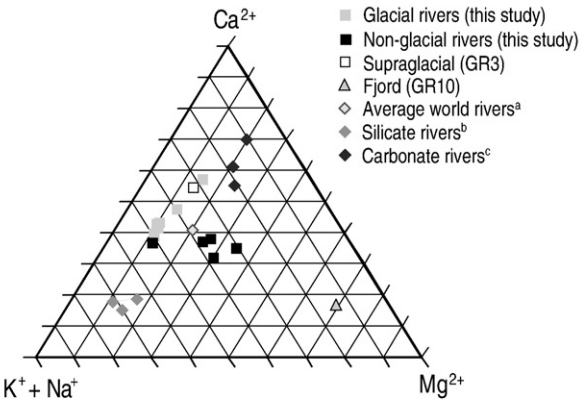

Fig. 2. Triplot diagram showing the major cation concentrations of the glacial and non-glacial rivers sampled in this study, as well as values for world rivers. [a]Average world river composition taken from Meybeck (2003). [b]Data for silicate dominated rivers taken from (Gaillardet et al. (1999b), Gislason et al. (1996) and Meybeck (1987). [c]Data for carbonate dominated rivers taken from Han and Liu (2004), Chen et al. (2002), and Galy et al. (1999).

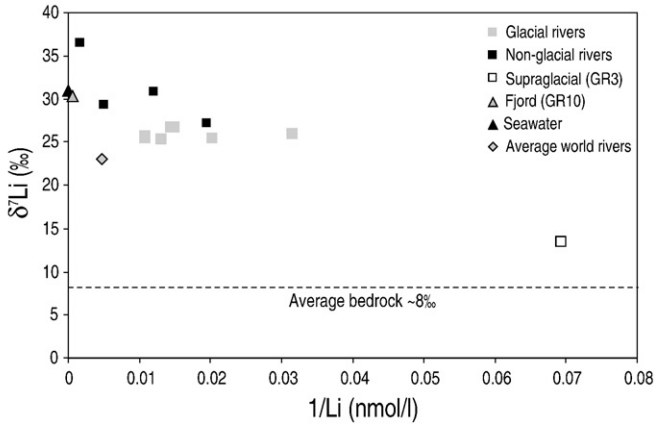

Fig. 3. Lithium concentration and isotope ratio (δ^7Li) of the dissolved load in the Greenland rivers. Value for average world rivers is from Huh et al. (1998).

lower levels of Li (between 8.8 and 13.5 ppm) and a lower average δ^7Li value (5‰). The suspended sediments have the highest concentrations of Li, containing on average 27 ppm Li which is more than twice the concentration found in the bedload. The suspended sediment always has a lower δ^7Li isotope ratio than the corresponding bedload; the average δ^7Li value of the suspended sediments is 3.5‰.

The concentration of Li in the dissolved load ranges from 14 nmol/l to 570 nmol/l; on average the Li concentration in the glacial rivers is ~60 nmol/l and in the non-glacial rivers it is ~180 nmol/l. The Li isotope composition of the dissolved load varies from 13.5 to 36‰. Most glacial rivers have a δ^7Li value close to ~26‰; sample GR3 (supraglacial) has more ^{6}Li (δ^7Li = 13.5‰) while non-glacial rivers tend to have higher δ^7Li values, ranging from 27.1 to 36.5‰ (Fig. 3).

The ultrafiltered phase has slightly lower Li concentrations than the dissolved (<0.2 μm) phase but the Li isotopic composition of both phases is similar. However, while colloids from non-glacial rivers have Li isotope ratios that are close to those in the dissolved load, colloids from glacial rivers have Li isotope ratios that are always lower than the corresponding dissolved load.

5. Discussion

5.1. Physical and chemical erosion rates

Relative to the non-glacial rivers, the glacial rivers carry substantial amounts of fine grained sediment (on average 0.5 g/l compared to ~0.01 g/l in non-glacial rivers) partly because of glacial grinding of the ice sheet on the underlying bedrock, producing abundant fine grained sediment, and partly because of the high discharge rates of the glacial rivers, enhancing their ability to transport this suspended sediment. On the other hand, the glacial rivers have lower TDS (10.5 μScm^{-1}) compared to the global riverine average [50 μScm^{-1}; (Gaillardet et al., 1999b)]. This is because the main source of water is surface or subsurface melting of glacial ice (Anderson et al., 2000; Tranter, 2003; Das et al., 2008) that has had limited contact with the bedrock (Anderson et al., 1997).

The Watson River is estimated to discharge 2.5 million tonnes of water annually, from April to September (Danish Polar Centre, 2008). Although concentrations of TDS and TSS are likely to vary throughout the melt season [e.g. (Statham et al., 2008)], the average values for TDS and TSS obtained in this study can be combined with these discharge data to give a crude estimate of annual weathering fluxes for the Watson River catchment. Using our average TDS value of 3.2 mg/l, the chemical weathering flux is ~8000 t yr^{-1} and using our average TSS value of 0.5 g/l the physical weathering flux is 1 250 000 t yr^{-1}. Calculation of chemical and physical weathering rates requires an estimate of the discharge area. In the present case

this is difficult to evaluate because some weathering will be occurring under the ice, and the extent of the subglacial catchment is not known. The deglaciated catchment of the Watson River drains an estimated 600 km^2 (Schjott, 2001) but the river is fed by Russell's Glacier and an unnamed glacier to the south. If it is assumed that surface melting and transfer of water englacially to the base of these glaciers extends ~20 km inland from the ice sheet margin (Tranter, 2003), then the size of the Watson River catchment increases by 200 km^2 giving a total catchment area of ~800 km^2. In addition, because the chemical composition of the glacial rivers is essentially constant, regardless of distance from the ice sheet, we also assume that the average concentrations of TDS and TSS in the subglacial zone are the same as those in the glacial rivers. Considered together, these data provide a rough estimate for chemical and physical erosion rates of 10 t/km^2/yr and 1560 t/km^2/yr, respectively. The value for the chemical erosion rate around Kangerlussaq is comparable to those calculated for other glaciated environments (West et al., 2005) but it is are lower than the global average chemical erosion rate [24 t/km^2/yr; (Gaillardet et al., 1999b)]. Relative to low-lying rivers that are unaffected by glacial processes, the rate of physical erosion in the Watson River catchment is high; for example physical erosion rates in the Seine, MacKenzie and Changjiang catchments are 9, 55, and 265 t/km^2/yr respectively (Gaillardet et al., 1999a,b). By comparison, the physical erosion rate that we calculate for the Watson River catchment is closer to rates calculated for rapidly eroding mountainous environments such as the East Southern Alps or Lesser Himalaya (Jacobson and Blum, 2003; West et al., 2005) and other glacial catchments, including Iceland where the average physical erosion rate is 1075 t/km^2/yr (Pogge von Strandmann et al., 2006).

5.2. Chemistry of glacial vs non-glacial rivers

The pH of natural waters is regulated by; a) the consumption of protons during the weathering of silicate rocks, and b) the production of protons by atmospheric CO_2 entering solution or the oxidation of sulphides (Galy et al., 1999). The low pH of the supraglacial sample (GR3, pH 6.3) is a result of this water having had no contact with the bedrock so proton consumption has only occurred via the interaction of meltwater with sediment entrained within the ice or added from aerosols. The glacial rivers have higher pH (7.1 to 8.4) and, in theory, subglacial weathering of silicates and carbonates could increase pH to >9, but this is mediated by the subglacial oxidation of sulphides which creates protons (Tranter, 2003). The pH of the glacial rivers thus reflects the combined effects of these processes. In the non-glacial rivers the pH of the water tends to reflect the amount of chemical weathering; for example sample GR12 has both high pH and TDS (8.3 and 200 μScm^{-1} respectively) indicating proton consumption during weathering reactions. Conversely sample GR11 has low pH and TDS (6.8 and 25 μScm^{-1} respectively) indicating that the chemical weathering intensity is relatively low and uptake of CO_2 from the atmosphere plays a more important role in controlling pH.

The major cation concentration of glacial rivers is dominated by Ca^{2+} (Fig. 2). This is in common with most glacial rivers, irrespective of the underlying lithology, and is due to the rapid dissolution kinetics of Ca^{2+} from trace carbonates and aluminosilicates (Anderson et al., 1997; Tranter, 2003). The glacial rivers also have a relatively high proportion of K^+ (~12%) because of non-stoichiometric dissolution of biotite and the leaching of interlayer K^+, a process that is relatively rapid under glaciers and in glacial soils (Newman and Brown, 1969; Blum et al., 1998). In non-glacial rives concentrations of TDS are higher, so preferential leaching of trace phases is less important and the relative proportion of K^+ is lower.

Glacial rivers contain relatively high levels of SO_4^{2-} (~22% of the total anion content) compared to non-glacial rivers (~10%) because of oxidation of trace sulphides in the subglacial environment [e.g. (Tranter et al., 2002)]. The glacial rivers have very low levels of Cl^- (~3% of the total cation content) and an average Cl^-/Na^+ ratio of 0.2, which is far lower than seawater (1.8). The relative importance of Cl^- is higher in the non-glacial rivers (~20%) because of high levels of evaporation (Anderson et al., 2001).

5.3. Lithium and lithium isotope systematics

The average δ^7Li value of glacial riverwater (~26‰) is slightly lower than the average value for non-glacial rivers (~30‰) but both types of rivers fall within the global range of riverine δ^7Li [6–41‰; (Huh et al., 1998; Kisakurek et al., 2005; Pogge von Strandmann et al., 2006)]. The δ^7Li value of the rocks from which the dissolved Li is derived is ~8‰, which means either that ^{6}Li has been preferentially removed from solution into secondary mineral phases, or that ^{7}Li is preferentially removed during dissolution of primary minerals. Experimental work on basalts (Pistiner and Henderson, 2003) shows that fractionation of Li isotopes is unlikely to occur during dissolution of primary phases, but a number of studies have shown that Li isotope fractionation occurs during the formation of secondary minerals [e.g. (Chan et al., 1992; Huh et al., 1998; Chan and Hein, 2007)].

The potential for secondary mineral formation can be assessed by calculating the saturation indices in solution using geochemical modelling software such as PHREEQC (Parkhurst and Appelo, 1999). The saturation index (SI) provides information about the stability of a mineral in solution; if the SI of a mineral is <0 then the mineral is undersaturated and will dissolve. If the SI is >0 then the mineral is oversaturated and has potential to precipitate. A value of 0 indicates that the mineral and solution are in equilibrium.

Comparison of cation concentrations for the dissolved and ultrafiltered fractions (Table 2) indicates that colloids are present in all of the river samples. As the stability of secondary minerals depends only on the concentration of truly dissolved species, SI values must be calculated using data for ultrafiltered waters. The results of these calculations show that the non-glacial rivers have, on average, slightly higher SI values than the glacial rivers but the difference for most minerals is small. Primary minerals, including diopside and albite, are always undersaturated in solution. With the exception of K-mica, most clay minerals are also undersaturated in both types of river systems. X-ray diffraction (XRD) analyses of the suspended load of glacial rivers support these calculations: results show that the sediments are mainly composed of plagioclase, amphibole and quartz (i.e. rock flour), and there are no obvious traces of crystalline secondary clays. However, in non-glacial rivers, PHREEQC modelling does suggest that iron oxyhydroxide minerals are oversaturated whereas they tend to be undersaturated in most glacial rivers (Fig. 4).

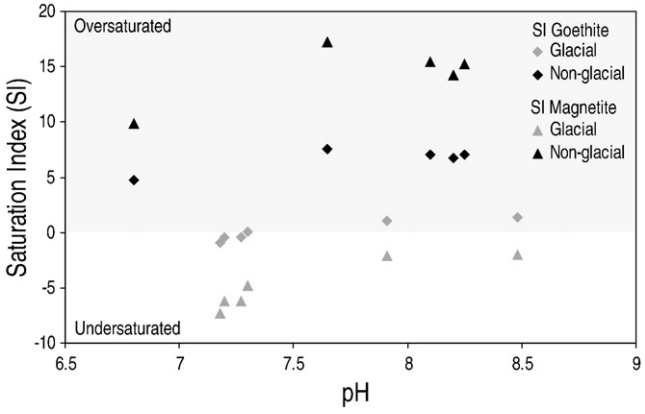

Fig. 4. Saturation indices of goethite and magnetite in the glacial and non-glacial rivers as a function of pH. All saturation indices have been calculated using the geochemical modelling software PHREEQC (Parkhurst and Appelo, 1999).

This is because all of the iron in solution in glacial rivers is actually colloidal (Table 2) whereas in the non-glacial rivers a significant proportion of Fe is present in the truly dissolved phase (<10 kD).

Solid-state NMR spectroscopy studies of iron oxyhydroxide minerals provide evidence for the formation of inner sphere Li^+ complexes on the iron oxyhydroxide surface (Nielsen et al., 2005; Kim et al., 2008). Crucially, inner sphere sorption appears to lead to fraction of Li isotopes with preferential uptake of ^6Li (Pistiner and Henderson, 2003; Chan and Hein, 2007). Thus, the high δ^7Li value of non-glacial river water is consistent with uptake of ^6Li by iron oxyhydroxide minerals. However, given that we have scant evidence for the formation of iron oxyhydroxides (or clay minerals) in the glacial rivers, the cause of high δ^7Li in these rivers demands a different explanation.

Could high δ^7Li values in the dissolved phase of glacial rivers be due to the presence of colloids? Clearly, the answer is 'no', for two reasons. Firstly, the amount of Li in colloidal form is very small (Table 2) and secondly, colloids in glacial rivers are always enriched in ^6Li (and not ^7Li) relative to truly dissolved Li (Fig. 5). Nevertheless, the data shown in Fig. 5 reveal important differences in the behaviour of Li and Li isotopes during glacial vs non-glacial weathering that warrants further discussion. In non-glacial rivers, the δ^7Li value of the colloidal fraction is the same as that of the dissolved or ultrafiltered fractions. In these rivers (some of which are notably coloured), the colloidal fraction is likely to consist mainly of humic or fulvic acids (Gaillardet et al., 2003), which would suggest that lithium is taken up by the organic colloids in a way that is indiscriminate of mass. On the other hand, in the glacial rivers, colloids are more likely to consist of ultrafine particles of bedrock that have been ground down by the glacier. The δ^7Li value of these colloids is always lower than that of the corresponding dissolved or ultrafiltered phases, and approaches the δ^7Li value of the bedrock (5.77–10.4‰; Table 3).

Although PHREEQC modelling indicates that the glacial rivers are undersaturated with respect to most clay minerals and Fe-oxyhydroxides, and XRD analyses of the suspended sediment are unable to identify any clay mineral component, the chemical composition of the suspended load is distinctly different from that of the bedrock and bedload. The suspended sediments tend to have higher Ca, Mg, K and Fe and lower Al, and they are strongly enriched in Li (~29 ppm, *cf* ~11 ppm in the bedload) and have lower δ^7Li (~3.3‰, *cf* ~5.3‰ in the bedload). One possibility is that the suspended sediments have been affected by processes occurring in the subglacial environment. This is because high concentrations of dissolved sulphate in the glacial rivers indicate that oxidation of sulphides has occurred where comminuted bedrock is first in contact with water (Wadham et al., 2007); crucially, a by product of this reaction is the formation of Fe-oxyhydroxides (Bottrell and Tranter, 2002; Tranter, 2003; Statham et al., 2008; Raiswell et al., 2009):

$$4Fe_2S + 16Ca_{(1-x)}Mg_xCo_3 + 15O_2 + 14H_2O \Rightarrow 16(1-x)Ca^{2+} + 16xMg^{2+} + 16HCO_3^- + 8SO_4^{2-} + 4Fe(OH)_3 \quad (1)$$

These Fe-oxyhydroxides are likely to nucleate on the comminuted bedrock (Raiswell et al., 2006) which is fine grained and thus held in suspension; in this connection, the suspended particles contain nearly twice as much Fe as the corresponding bedload (Table 3). As discussed above, the freshly precipitated iron oxyhydroxide particles are likely to adsorb Li^+ ions from solution. The results of our leaching experiments support this idea (Fig. 6). Only 2% of available Li (and 0.5% of available Fe) is loosely-bound (i.e. removed by leaching in acetate buffer solution), but ~65% of the Li in the suspended particles appears to be associated with Fe-oxyhydroxide phases (i.e. released by leaching in 2N HCl). Moreover, the δ^7Li value of this Li (~5‰) is far lower than the δ^7Li value of the dissolved phase (~25‰) which suggests that ^6Li is taken up in preference to ^7Li. Loosely-bound Li also has a lower δ^7Li value (~15‰) than the dissolved phase; this is surprising, because the Li is likely to be bonded to the particles by electrostatic attractions, which have no isotopic preference (Pistiner and Henderson, 2003; Chan and Hein, 2007). Rather, we suggest that the acetate buffer leach may have released a small amount of Li that is associated with poorly crystalline Fe-oxyhydroxides.

The fractionation factor between the isotope ratio of Li associated with Fe-oxyhydroxides and Li in the ultrafiltered riverwater ($\alpha_{mineral-fluid}$) is 0.980. This is a slightly greater fractionation factor than that calculated by Pistiner and Henderson (2003) for the formation of inner sphere Li^+ complexes on the surface of gibbsite ($\alpha = 0.986$) but it is within the range of values reported for Li uptake from seawater into ferromanganese crusts [$\alpha = 0.978–0.999$; (Chan and Hein, 2007)]. It is also similar to values obtained by (Zhang et al., 1998) in a study of Li uptake from seawater onto kaolinite and vermiculite ($\alpha = 0.979$ and 0.971, respectively).

While Li appears to be strongly affected by processes occurring in the subglacial environment, the Li concentration and Li isotopic composition of riverwater changes very little as it flows from the head of the glacier (Sample GR1) to a sampling point located 30 km downstream (Sample GR5). This suggests that little Li is added by dissolution of primary minerals (presumably because water-rock contact time is short and temperature is low), and little Li is removed into secondary phases as these phases are undersaturated and thus unlikely to form in the river itself.

5.4. Glacial weathering: effects on the Li and Li isotope composition of global runoff

The quantity and distribution of runoff from glaciated and non-glaciated terrain have varied considerably in the past (e.g. Roberts et al., 2009), and are predicted to do so in the future (e.g. Fichefet et al., 2003). In this study, we have shown that the Li isotopic composition of glacial runoff is lighter than that of non-glacial runoff from the same terrain (respectively, $\delta^7Li = 26‰$ versus $\delta^7Li = 30‰$; Table 2); this is also consistent with data for glacial and non-glacial rivers in Iceland, which drain basalt (Pogge von Strandmann et al., 2006). However, because glacial rivers have low [Li] and, at present, runoff from ice sheets constitutes only ~1% of total global runoff (Jones et al., 2002), the 4‰ offset in δ^7Li values between glacial and non-glacial rivers has a negligible (<0.01‰) effect on the δ^7Li of runoff at the global scale. Nevertheless, at the height of the last deglaciation, the total global runoff was ~55×10^3 km^3 yr^{-1} (some 22% higher than it is today) and the glacial flux consisted of ~18% of the total (Jones et al., 2002). In this case, in the very simplest sense and assuming that non-glacial rivers have Li concentration and δ^7Li values close to today's global average (respectively, 215 nM and $\delta^7Li = 23‰$ (Huh et al., 1998)), and that glacial rivers have a Li concentration of 68 nM

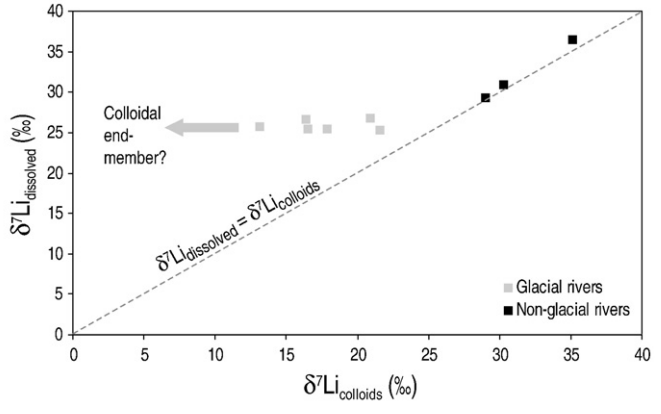

Fig. 5. A comparison of the lithium isotope ratio in the dissolved load (<0.2 μm) and the colloidal phase (<0.2 μm, >10 kD).

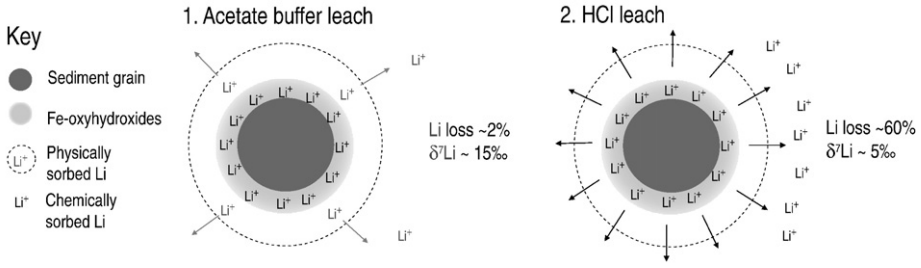

Fig. 6. Schematic diagram showing the two step leaching process adopted for the suspended sediments and the concentration and isotope ratio of Li derived from each leach.

and a δ^7Li value that is 4‰ lower than that of non-glacial rivers (this study), then mass balance indicates that the Li isotope composition of the global river flux was still only ~0.3% lower than it would have been if there was no glacial runoff. This offset is within the external reproducibility of Li isotope measurements (e.g. see Section 3.4).

In the same connection, the results of this study indicate that in glacial rivers, ~65% (≈18 ppm) of the lithium in suspended sediments is associated with Fe-oxyhydroxide phases. Given a physical weathering flux from the Watson River catchment of ~1 250 000 t yr^{-1} (Section 5.1), this constitutes a Li flux of 22.5 kg yr^{-1}, which is an order of magnitude greater than the flux of dissolved Li (1.1 kg yr^{-1}). Thus, Li associated with Fe-oxyhydroxide phases potentially represents a significant flux of Li to the oceans, that has a very different isotopic composition to the dissolved riverine signal. Moreover, recent work on suspended sediments from glacial meltwaters, supraglacial and proglacial sediments, and sediments in basal ice, from Arctic, Alpine and Antarctic locations, has revealed that Fe-oxyhydroxide phases are ubiquitous in glacial settings (Raiswell et al., 2006). The question is, what proportion of this material reaches the open ocean, and how much of it actually dissolves? Raiswell et al. (2006) point out that while the sediment flux from icebergs is transferred directly into the open ocean, much of the sediment flux carried by meltwater runoff is likely to be physically trapped in fjords, and only ~10% of this material is transferred. To our knowledge, there are no data concerning the solubilisation of Li associated with Fe-oxyhydroxide phases in seawater. However, there are a number of studies on Fe solubility; for example, 0 to 87% of total Fe delivered to the oceans in aeolian dust may be solubilised (Hand et al., 2004), while 5–10% of nanoparticulate Fe in ice-hosted sediment is estimated to be bioavailable (Raiswell et al., 2008). Table 4 estimates the potential global flux of Li due to solubilisation of Fe-oxyhydroxides, utilising sediment fluxes for the present day and also for the Last Glacial Maximum (LGM) estimated by Raiswell et al. (2006). Relative to today's global dissolved riverine Li flux (8×10^9 mol/yr; Huh et al., 1998), this flux is small (<5%), even if Li solubilisation is extreme (10%). Moreover, the effect on the δ^7Li value of global runoff is small (<0.8‰). Even at the LGM, when fluxes of glacially derived sediment were substantially larger (Table 4), the flux of Li derived from glacial sediment is only significant (>10% of the dissolved riverine flux) if the level of Li solubilisation is extreme. In order to confirm these results, experiments concerning the solubilisation of Li from Fe-oxyhydroxide particles at seawater pH are required, but it seems likely that, on the global scale, this is not an important source of Li to the oceans, even when sediment fluxes are high (e.g. LGM).

These flux calculations have implications for the potential use of Li and Li isotopes as proxies for silicate weathering (Kisakurek et al., 2005; Hathorne and James, 2006), and in turn as proxies for atmospheric CO_2 consumption rates [e.g. (Gaillardet et al., 1999b)]. Crucially, they demonstrate that the flux of Li from glacial rivers is small; <6% of the total river input at the height of the last deglaciation and <0.2% of the total river input today. This result is important because, under the glacier bed, weathering of some silicate minerals, such as K-feldspar which can be rich in Li, can occur via hydrolysis rather than carbonation (Tranter et al., 2002). Release of Li from silicates via hydrolysis does not involve sequestration of atmospheric CO_2; if this study had demonstrated that this process was an important source of Li, the relationship between Li, silicate weathering and atmospheric CO_2 would be invalidated.

Table 4
Global glacial sediment and Li fluxes. [a]Total flux to the open ocean assumes that 10% of meltwater runoff reaches the open ocean. Amount of Li associated with Fe-oxyhydroxide phases is 18 ppm (this study); Li fluxes are calculated for dissolution of 0.1, 1 and 10% of this phase. Sediment fluxes are from Raiswell et al. (2006).

	Present day				LGM			
	Sediment flux (Tg yr^{-1})	Li flux (10^9 mol yr^{-1})			Sediment flux (Tg yr^{-1})	Li flux (10^9 mol yr^{-1})		
		0.1%	1%	10%		0.1%	1%	10%
Meltwater runoff	1400	0.004	0.04	0.36	6000	0.02	0.16	1.56
Iceberg calving	1450	0.004	0.04	0.38	5250	0.01	0.14	1.36
Total flux to open ocean[a]	1590	0.004	0.04	0.41	5310	0.01	0.14	1.38

6. Conclusions

The chemical composition of glacial rivers from West Greenland differs from that of its non-glacial rivers. The glacial rivers contain a higher proportion of dissolved Ca^{2+} and K^+ because of preferential weathering of trace carbonates and biotite, and they have higher SO_4^{2-} because of oxidation of trace sulphides under the ice. Levels of total dissolved solids are low, and levels of total suspended solids are high, in the glacial rivers (respectively, 10.5 μScm^{-1} and 0.5 g l^{-1} in the glacial rivers compared to 100 μScm^{-1} and 0.01 g l^{-1} in the non-glacial rivers).

The average δ^7Li value of glacial riverwater (~26‰) is slightly lighter than the average for non-glacial rivers (~30‰). These values are significantly different from those of the rocks from which the dissolved Li is derived (~8‰), suggesting that ^{6}Li has been preferentially removed from solution into secondary mineral phases. Saturation state modelling predicts that Fe-oxyhydroxide phases are supersaturated and thus likely to form in the non-glacial rivers. Inner sphere sorption of Li^+ is known to occur on the surface of Fe-oxyhydroxides; these data therefore suggest that this process leads to fraction of Li isotopes with preferential uptake of ^{6}Li.

XRD analyses and saturation state modelling provide scant evidence for the formation of clay minerals or Fe-oxyhydroxides in glacial rivers however. Rather, we suggest that fractionation of Li isotopes occurs under the ice, via uptake of Li on Fe-oxyhydroxide minerals that form as a product of sulphide oxidation. This is supported by analysis of the suspended sediments, which reveals that ~65% of the Li in the sediments is associated with Fe-oxyhydroxide phases. Moreover, the δ^7Li value of this Li (~5‰) is far lower than the δ^7Li value of the dissolved phase (~26‰) which suggests that ^{6}Li is taken up in preference to ^{7}Li.

Because the difference between the δ^7Li values of glacial vs non-glacial rivers is small, glaciation has not had a significant impact on the Li isotopic composition of the global riverine flux of Li delivered to the oceans in the past. Moreover, the flux of Li delivered to the oceans via glacial rivers is small, <6% of the total even at the height of the last deglaciation. This means that weathering of Li via processes that are not linked to sequestration of atmospheric CO_2 is not significant.

Acknowledgements

We would like to thank the Danish Polar Centre and the Greenland government for giving us permission to undertake our fieldwork and we thank the staff of the Kangerlussuaq International Science Support (KISS) facility for their invaluable logistical support. We also thank Phil Pogge von Strandmann for help in the field, and John Watson for assistance with XRF analyses. The manuscript benefited from the constructive comments and suggestions of two anonymous reviewers. JW's PhD studentship was funded by the UK Natural Environment Research Council (NE/B502701/1).

References

Anderson, S.P., Drever, J.I., Humphrey, N.F., 1997. Chemical weathering in glacial environments. Geology 25, 399–402.
Anderson, N.J., Bennike, O., Christofferson, K., Jeppesen, E., Markager, S., Miller, G., Renberg, I., 1999. Limnological and palaeolimnological studies of lakes in south-western Greenland. Geol. Greenland Surv. Bull. 185, 68–74.
Anderson, S.P., Drever, J.I., Frost, C.D., Holden, P., 2000. Chemical weathering in the foreland of a retreating glacier. Geochim. Cosmochim. Acta 64, 1173–1189.
Anderson, N.J., Harriman, R., Ryves, D.B., Patrick, S.T., 2001. Dominant factors controlling variability in the ionic composition of West Greenland lakes. Arct. Antarct. Alp. Res. 33, 418–425.
Appelo, C.A.J., Postma, D., 2005. Geochemistry, Groundwater and Pollution. A.A. Balkema. 649 pp.
Berner, R.A., Lasaga, A.C., Garrels, R.M., 1983. The carbonate–silicate geochemical cycle and its effect on atmospheric carbon-dioxide over the past 100 million years. Am. J. Sci. 283, 641–683.
Blum, J.D., Gazis, C.A., Jacobson, A.D., Chamberlain, C.P., 1998. Carbonate versus silicate weathering in the Raikhot watershed within the high Himalayan crystalline series. Geology 26, 411–414.
Bottrell, S.H., Tranter, M., 2002. Sulphide oxidation under partially anoxic conditions at the bed of the Haut Glacier d'Arolla, Switzerland. Hydrol. Process. 16, 2363–2368.
Bryden, H.L., Longworth, H.R., Cunningham, S.A., 2005. Slowing of the Atlantic meridional overturning circulation at 25°N. Nature 438, 655–657.
Chan, L.H., Hein, J.R., 2007. Lithium contents and isotopic compositions of ferromanganese deposits from the global ocean. Deep-Sea Res. Part II-Top. Stud. Oceanogr. 54, 1147–1162.
Chan, L.H., Edmond, J.M., Thompson, G., Gillis, K., 1992. Lithium isotopic composition of submarine basalts — implications for the lithium cycle in the oceans. Earth Planet. Sci. Lett. 108, 151–160.
Chen, J., Wang, F., Xia, X., Zhang, L., 2002. Major element chemistry of the Changjiang (Yangtze River). Chem. Geol. 187, 231–255.
Danish Polar Centre 2008, International Polar Year (IPY), www.ipy.dk
Das, S.B., Joughin, I., Behn, M.D., Howat, I.M., King, M.A., Lizarralde, D., Bhatia, M.P., 2008. Fracture propagation to the base of the Greenland Ice Sheet during supraglacial lake drainage. Science 320, 778–781.
Dupre, B., Viers, J., Dandurand, J.L., Polve, M., Benezeth, P., Vervier, P., Braun, J.J., 1999. Major and trace elements associated with colloids in organic-rich river waters: ultrafiltration of natural and spiked solutions. Chem. Geol. 160, 63–80.
Escher, J.C., Pulvertaft, T.C.R., 1995. Geological Map of Greenland 1:2500000, Geological Survey of Denmark and Greenland (GEUS), Copenhagen.
Fichefet, T., Poncin, C., Goosse, H., Huybrechts, P., Janssens, I., Le Treut, H., 2003. Implications of changes in freshwater flux from the Greenland ice sheet for the climate of the 21st century. Geophys. Res. Lett. 30, 1911. doi:10.1029/2003GL017826.
Flesch, G.D., Anderson, A.R., Svec, H.J., 1973. A secondary isotopic standard for 6Li/7Li determinations. Int. J. Mass Spectrom. Ion Phys. 12, 265–272.
Gaillardet, J., Dupre, B., Allegre, C.J., 1999a. Geochemistry of large river suspended sediments: silicate weathering or recycling tracer? Geochim. Cosmochim. Acta 63, 4037–4051.
Gaillardet, J., Dupre, B., Louvat, P., Allegre, C.J., 1999b. Global silicate weathering and CO2 consumption rates deduced from the chemistry of large rivers. Chem. Geol. 159, 3–30.
Gaillardet, J., Viers, J., Dupre, B., 2003. Trace Elements in River Waters. In: Holland, H.D., Turekian, K.K. (Eds.), Treatise on Geochemistry. Pergamon, Oxford, pp. 225–272.
Galy, A., France-Lanord, C., Derry, L.A., 1999. The strontium isotopic budget of Himalayan rivers in Nepal and Bangladesh. Geochim. Cosmochim. Acta 63, 1905–1925.
Gislason, S.R., Arnorsson, S., Armannsson, H., 1996. Chemical weathering of basalt in southwest Iceland: effects of runoff, age of rocks and vegetative/glacial cover. Am. J. Sci. 296, 837–907.
Han, G., Liu, C.-Q., 2004. Water geochemistry controlled by carbonate dissolution: a study of the river waters draining karst-dominated terrain, Guizhou Province, China. Chem. Geol. 204, 1–21.
Hand, J.L., Mahowald, N.M., Chen, Y., Siefert, R.L., Luo, C., Subramaniam, A., Fung, I., 2004. Estimates of atmospheric-processes soluble iron from observations and a global mineral aerosol model: biogeochemical implications. J. Geophys. Res. 109, D17205. doi:10.1029/2004JD004574.
Hathorne, E.C., James, R.H., 2006. Temporal record of lithium in seawater: a tracer for silicate weathering? Earth Planet. Sci. Lett. 246, 393–406.
Huh, Y., Chan, L.H., Zhang, L., Edmond, J.M., 1998. Lithium and its isotopes in major world rivers: implications for weathering and the oceanic budget. Geochim. Cosmochim. Acta 62, 2039–2051.
Huh, Y., Chan, L.H., Edmond, J.M., 2001. Lithium isotopes as a probe of weathering processes: Orinoco River. Earth Planet. Sci. Lett. 194, 189–199.
Jacobson, A.D., Blum, J.D., 2003. Relationship between mechanical erosion and atmospheric CO2 consumption in the New Zealand Southern Alps. Geology 31, 865–868.
James, R.H., Palmer, M.R., 2000. The lithium isotope composition of international rock standards. Chem. Geol. 166, 319–326.
Jones, I.W., Munhoven, G., Tranter, M., Huybrechts, P., Sharp, M.J., 2002. Modelled glacial and non-glacial HCO3−, Si and Ge fluxes since the LGM: little potential for impact on atmospheric CO2 concentrations and a potential proxy of continental chemical erosion, the marine Ge/Si ratio. Glob. Planet. Change 33, 139–153.
Jorgensen, A.S., Andreasen, F., 2007. Mapping of permafrost surface using ground-penetrating radar at Kangerlussuaq Airport, western Greenland. Cold Reg. Sci. Technol. 48, 64–72.
Kim, J., Nielsen, U.G., Grey, C.P., 2008. Local environments and lithium adsorption on the iron oxyhydroxides lepidocrocite and goethite: a 2H and 7Li solid-state MAS NMR study. J. Am. Chem. Soc. 130, 1285–1295.
Kisakurek, B., Widdowson, M., James, R.H., 2004. Behaviour of Li isotopes during continental weathering: the Bidar laterite profile, India. Chem. Geol. 212, 27–44.
Kisakurek, B., James, R.H., Harris, N.B.W., 2005. Li and delta Li-7 in Himalayan rivers: proxies for silicate weathering? Earth Planet. Sci. Lett. 237, 387–401.
Meybeck, M., 1987. Global chemical-weathering of surficial rocks estimated from river dissolved loads. Am. J. Sci. 287, 401–428.
Meybeck, M., 2003. Global Occurrence of Major Elements in Rivers. In: Holland, H.D., Turekian, K.K. (Eds.), Treatise on Geochemistry. Pergamon, Oxford, pp. 207–223.
Newman, A.C.D., Brown, G., 1969. Delayed exchange of potassium from some edges of mica flakes. Nature 223, 175–176.
Nielsen, U.G., Paik, Y., Julmis, K., Schoonen, M.A.A., Reeder, R.J., Grey, C.P., 2005. Investigating sorption on iron oxyhydroxide soil minerals by solid-state NMR spectroscopy: a 6Li MAS NMR study of adsorption and absorption on goethite. J. Phys. Chem. B 109, 18310–18315.
Parkhurst, D.L., Appelo, C.A.J., 1999. User's guide to PHREEQC (version 2) — a computer program for speciation, batch-reaction, one-dimensional transport, and inverse geochemical calculations. U.S. Geological Survey Water-Resources Investigations Report, p. 312.
Petrovich, R., 1981. Kinetics of dissolution of mechanically comminuted rock-forming oxides and silicates in the laboratory and at the Earth's surface. Geochim. Cosmochim. Acta 45, 1675–1686.
Pistiner, J.S., Henderson, G.M., 2003. Lithium-isotope fractionation during continental weathering processes. Earth Planet. Sci. Lett. 214, 327–339.
Pogge von Strandmann, P.A.E., Burton, K.W., James, R.H., van Calsteren, P., Gislason, S.R., Mokadem, F., 2006. Riverine behaviour of uranium and lithium isotopes in an actively glaciated basaltic terrain. Earth Planet. Sci. Lett. 251, 134–147.
Raiswell, R., Thomas, A.G., 1984. Solute acquisition in glacial melt waters. 1. Fjallsjokull (southeast Iceland) — bulk melt waters with closed-system characteristics. J. Glaciol. 30, 35–43.
Willemse, N., 2002. Holocene sedimentation history of the shallow Kangerlussuaq lakes, West Greenland, Meddelelser om Gronland. Geosience 41, 1–48.
Raiswell, R., Tranter, M., Benning, L.G., Siegert, M., De'ath, R., Huybrechts, P., Payne, T., 2006. Contributions from glacially derived sediment to the global iron (oxyhydr) oxide cycle: implications for iron delivery to the oceans. Geochim. Cosmochim. Acta 70, 2765–2780.
Raiswell, R., Benning, L., Davidson, L., Tranter, M., 2008. Nanoparticulate bioavailable iron minerals in icebergs and glaciers. Mineral. Mag. 72, 345–348.
Raiswell, R., Benning, L., Davidson, L., Tranter, M., Tulaczyk, S., 2009. Schwertmannite in wet, acid, and oxic microenvironments beneath polar and polythermal glaciers. Geology 37, 431–434.
Riotte, J., Chabaux, F., Benedetti, M., Dia, A., Gerard, M., Boulegue, J., Etame, J., 2003. Uranium colloidal transport and origin of the U-234-U-238 fractionation in surface waters: new insights from Mount Cameroon. Chem. Geol. 202, 365–381.
Roberts, D.H., Long, A.J., Schnabel, C., Davies, B.J., Xu, S., Simpson, M.J.R., Huybrechts, P., 2009. Ice sheet extent and early deglacial history of the southwestern sector of the Greenland Ice Sheet. Quat. Sci. Rev. 28, 2760–2773.
Russell, A.J., 2007. Controls on the sedimentology of an ice-contact jokulhlaup-dominated delta, Kangerlussuaq, west Greenland. Sediment. Geol. 193, 131–148.
Schjott, T., 2001. Sisimiut & Kangerlussuaq 1:250000, Saga Maps.
Sharp, M., Tranter, M., Brown, G.H., Skidmore, M., 1995. Rates of chemical denudation and CO2 drawdown in a glacier-covered Alpine catchment. Geology 23, 61–64.
Statham, P., Skidmore, M., Tranter, M., 2008. Inputs of glacially derived dissolved and colloidal iron to the coastal ocean and implications for primary productivity. Glob. Biogeochem. Cycles 22, GB3013.
Tranter, M., 2003. Geochemical Weathering in Glacial and Proglacial Environments. In: Holland, H.D., Turekian, K.K. (Eds.), Treatise on Geochemistry. Pergamon, Oxford, pp. 189–205.

Tranter, M., Huybrechts, P., Munhoven, G., Sharp, M.J., Brown, G.H., Jones, I.W., Hodson, A.J., Hodgkins, R., Wadham, J.L., 2002. Direct effect of ice sheets on terrestrial bicarbonate, sulphate and base cation fluxes during the last glacial cycle: minimal impact on atmospheric CO2 concentrations. Chem. Geol. 190, 33–44.

van de Flierdt, T., Frank, M., Lee, D.C., Halliday, A.N., 2002. Glacial weathering and the hafnium isotope composition of seawater. Earth Planet. Sci. Lett. 198, 167–175.

Vigier, N., Decarreau, A., Millot, R., Carignan, J., Petit, S., France-Lanord, C., 2008. Quantifying Li isotope fractionation during smectite formation and implications for the Li cycle. Geochim. Cosmochim. Acta 72, 780–792.

Wadham, J.L., Cooper, R.J., Tranter, M., Bottrell, S., 2007. Evidence for widespread anoxia in the proglacial zone of an Arctic glacier. Chem. Geol. 243, 1–15.

Walker, J.C.G., Hays, P.B., Kasting, J.F., 1981. A negative feedback mechanism for the long-term stabilization of Earth's surface-temperature. J. Geophys. Res.-Oceans Atmos. 86, 9776–9782.

Wells, P.R.A., 1979. Chemical and thermal evolution of Archaean sialic crust, southern West Greenland. J. Petrol. 20, 187–226.

West, A.J., Galy, A., Bickle, M., 2005. Tectonic and climatic controls on silicate weathering. Earth Planet. Sci. Lett. 235, 211–228.

White, A.F., Blum, A.E., 1995. Effects of climate on chemical-weathering in watersheds. Geochim. Cosmochim. Acta 59, 1729–1747.

Williams, L.B., Hervig, R.L., 2005. Lithium and boron isotopes in illite–smectite: the importance of crystal size. Geochim. Cosmochim. Acta 69, 5705–5716.

Yde, J.C., Knudsen, N.T., Nielsen, O.B., 2005. Glacier hydrochemistry, solute provenance, and chemical denudation at a surge-type glacier in Kuannersuit Kuussuat, Disko Island, West Greenland. J. Hydrol. 300, 172–187.

Zhang, L.B., Chan, L.H., Gieskes, J.M., 1998. Lithium isotope geochemistry of pore waters from ocean drilling program sites 918 and 919, Irminger Basin. Geochim. Cosmochim. Acta 62, 2437–2450.